Received 21 September 2025; Accepted 28 October 2025
https://doi.org/10.48612/letters/2025-4-350-354
https://elibrary.ru/xjxjgq

Determination of elastic properties of salt rocks using the four-point bending test

A. Yu. Fedorov†, E. B. Galkina, V. P. Matveenko, G. S. Serovaev

†fedorov@icmm.ru

Institute of Continuous Media Mechanics, Russian Academy of Sciences, Perm 614018, Russia

Abstract: The paper presents a method for determining the elastic moduli and Poisson's ratios of a material under compression and tension. The method is based on the results of strain measurements by fiber-optic sensors in a rectangular beam subjected to four-point bending. The relationships for determining the elastic moduli follow from an analytical solution for bending a rectangular beam made of a material with different moduli in compression and tension, assuming the Euler–Bernoulli hypothesis is satisfied. The relationships for determining Poisson's ratios follow from the assumption of a uniaxial stress state in the strain measurement zone. An algorithm is presented for estimating the errors in determining the elastic constants, which are due to deviations from the conditions of the Euler–Bernoulli hypothesis and a uniaxial stress state for the corresponding beam dimensions. Relations are presented for estimating the maximum errors in determining the elastic constants, based on the obtained relationships for their determination, associated with the error in measuring strains by the fiber-optic sensors used. Options for attaching the fiber-optic sensors to the surface of the specimens are considered. For a set of rock salt samples, the results of determining the elastic moduli and Poisson's ratios are presented, along with estimates of the errors in their determination, due to strain measurement errors and sample dimensions. The qualitative results obtained for the elastic constants in compression and tension, taking into account their errors, allow to conclude that rock salt is not a bi-modulus material.

Keywords: salt rocks, rocks, strain measurement, Young's modulus, Poisson's ratio, numerical modeling, distributed and point fiber-optic sensors

Acknowledgements: *This work was supported by the Russian Science Foundation (Project No. 19-77-30008).*

1. Introduction

The mechanical characteristics of rocks, including rock salt, are essential for understanding their deformation behavior in various engineering applications. Rock salt has unique physical and mechanical properties, including plasticity, creep, low porosity and permeability, and the ability to undergo significant deformations without failure [1–3]. Despite the complex nature of its mechanical behavior, elastic constants are among the main characteristics that determine the deformation behavior of rock salt. For example, in [4] it is noted that the elastic modulus and Poisson's ratio are the most important parameters for describing the elastic behavior of rock salt. In [5] it is noted that these parameters provide important information about the properties of the formation, as they are related to strain characteristics. Most studies on measuring the strength and mechanical characteristics of salt rocks are based on static tests under uniaxial compression [6,7]. The history of work in this area includes early measurements of stress-strain relationships using rigid testing machines and the subsequent use of servo-controlled testing machines, which record the stress-strain relationship with higher accuracy [8].

In laboratory compression tests on salt rocks, it is important to account for the influence of friction between the specimen and the surfaces of the testing machine on the measured strength and elastic modulus. Studies [9,10] have shown that reducing friction through lubrication or by selecting an optimal specimen height-to-diameter ratio decreases the measured parameters.

Since natural materials may exhibit different mechanical characteristics under compression and tension [11,12], a reliable assessment of the elastic behavior of salt rocks requires information on the tensile modulus of elasticity. However, testing rock salt specimens under uniaxial tension is highly labor-intensive, as it requires rigid fixation of the specimen ends in steel grips [13]. This has led to the development of several indirect methods, such as the Brazilian disk splitting method or splitting a disk with wedges [14]. In [14], a comparison of the results of the direct method (specimen rupture) and the indirect method (splitting the disk with coaxial wedges) for salt rocks is presented, demonstrating that the difference in the results obtained by different methods is by no more than a few percent. Thus, indirect methods are more commonly used to estimate the tensile modulus of elasticity, while Poisson's ratio under tension is usually assumed to be equal to that under compression.

To determine the mechanical properties of rocks, three- and four-point bending methods are also used, with specimens in the form of beams of rectangular or circular cross-section [15,16]. However, these studies are generally limited to assessing only the ultimate strength and strain characteristics of rocks [15,17].

Dynamic methods propose to determine elastic properties based on acoustic wave velocity. These methods provide continuous profiles of elastic parameters and allow for determining mechanical properties in formations where core samples may be unavailable [18,19].

In addition to direct experiments, numerical methods for assessing the mechanical characteristics of salt formations are used, which are associated with solving inverse problems, namely, determining the parameters of the material's mechanical behavior model that ensure the experimentally measured strains are obtained when calculating the stress-strain state of the selected object.

An analysis of the methods for determining the elastic constants of rocks, including rock salt, shows that each has its advantages and limitations. In this work, a four-point bending scheme is considered for determining Young's moduli and Poisson's ratios of rock salt in compression and tension, which complements the capabilities of existing methods for determining elastic constants.

2. Determination of elastic constants in four-point bending tests of rectangular specimens

In four-point bending tests, it is possible to simultaneously obtain tensile and compressive strains on a single specimen under the same physical environmental parameters. In the classic variants of four-point bending of rectangular beams with constant cross-section, the deflection and bending moment are measured. Then, based on these values, the elastic modulus and ultimate strengths are obtained for materials with identical behavior in compression and tension.

In the considered variant of four-point bending of rectangular beams (Fig. 1), for a given bending moment $M = PL/4$, the longitudinal ε_x and transverse ε_y strains are measured at the center of the top and bottom surfaces of the specimen, which correspond to compression and tension zones, respectively. Strains can be measured using single-point fiber-optic sensors based on Bragg gratings or distributed fiber-optic sensors based on Rayleigh scattering [20].

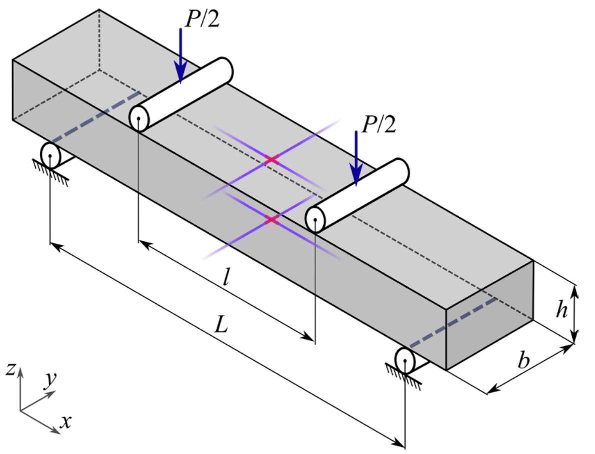

Fig. 1. The scheme of four-point bending test.

Measuring the two components of the strain tensor in the compression and tension zones opens the possibility to determine the material's elastic moduli and Poisson's ratios in compression and tension, respectively.

Analytical relations for calculating elastic constants based on experimental strain data of a beam under four-point bending, when beam material has linear-elastic behavior under tension and compression, can be obtained if two conditions are met. The distribution of longitudinal strains through the specimen thickness in the measurement zone must be linear, which corresponds to the Bernoulli–Euler hypothesis, and the stress–strain state must correspond to a uniaxial stress state. The first condition is the main requirement for obtaining an analytical solution for the bending of a beam. In [21] an analytical solution for the bending of a bi-modulus material beam with a linear stress–strain dependence in the compression and tension zones is provided, from which relations follow for calculating elastic moduli in tension and compression.

$$E^{+} = \frac{3M}{bh^2}\frac{\left(\varepsilon_x^{+} - \varepsilon_x^{-}\right)}{\left(\varepsilon_x^{+}\right)^2}, \quad E^{-} = \frac{3M}{bh^2}\frac{\left(\varepsilon_x^{+} - \varepsilon_x^{-}\right)}{\left(\varepsilon_x^{-}\right)^2}. \tag{1}$$

Satisfaction of the second condition makes it possible to calculate Poisson's ratios in tension ν^{+} and compression $\nu-$.

$$\nu^{+} = -\varepsilon_y^{+}/\varepsilon_x^{+}, \quad \nu^{-} = -\varepsilon_y^{-}/\varepsilon_x^{-}. \tag{2}$$

Here ε_x^{+}, ε_y^{+}, ε_x^{-}, ε_y^{-} are the measured strains on the specimen surfaces in the tension (+) and compression (–) zones, respectively.

3. Estimation of errors in determining elastic constants in compression and tension based on four-point bending test

The error in determining elastic constants in four-point bending test is governed by two main factors. The first is associated with the error in strain measurement by fiber-optic sensors. From relations (1) and (2), the following expressions can be obtained for the maximum possible error in determining Poisson's ratios in the tension α_ν^{+} and compression α_ν^{-} zones

$$\alpha_\nu^{+} = \left|\frac{\left(\varepsilon_x^{+} - \varepsilon_y^{+}\right)\delta}{\left(\varepsilon_x^{+} - \delta\right)\varepsilon_y^{+}}\right| \cdot 100\%, \quad \alpha_\nu^{-} = \left|\frac{\left(\varepsilon_x^{-} - \varepsilon_y^{-}\right)\delta}{\left(\varepsilon_x^{-} - \delta\right)\varepsilon_y^{-}}\right| \cdot 100\% \tag{3}$$

and the maximum error in determining elastic moduli

$$\alpha_E = \left|1 - \frac{\varepsilon^2}{(\varepsilon - \delta)^2}\right| \cdot 100\%, \tag{4}$$

where δ is the strain measurement error of the fiber-optic sensors, $\varepsilon = \max\left\{\left|\varepsilon_x^{+}\right|, \left|\varepsilon_x^{-}\right|\right\}$.

Eqs. (3) and (4) are equivalent to the following quantities

$$\alpha_\nu = \left(\nu - \nu^{*}\right)/\nu \cdot 100\%, \quad \alpha_E = \left(E - E^{*}\right)/E \cdot 100\%.$$

where ν, E are obtained by Eqs. (1) and (2) by utilizing the strain values ε_x^{+}, ε_y^{+}, ε_x^{-}, ε_y^{-} without error δ; ν^*, E^* are obtained by utilizing the strain values ε_x^{+}, ε_y^{+}, ε_x^{-}, ε_y^{-} with error δ, which gives the largest difference from ν, E.

The second error factor is related to the dimensions of the specimen, which determine the deviations in the strain measurement zone from the conditions of a uniaxial stress state and the conditions corresponding to the Bernoulli–Euler hypothesis.

Errors in determining Young's modulus and Poisson's ratio for non-bimodular materials, associated with specimen dimensions, are proposed to be evaluated using the following relations:

$$\beta_\nu = (\nu_0 - \nu)/\nu_0 \cdot 100\%, \quad \beta_E = (E_0 - E)/E_0 \cdot 100\%, \qquad (5)$$

where ν_0, E_0 are the values of elastic constants used for numerical simulation of the four-point bending of the specimen within the framework of the three-dimensional theory of elasticity; ν, E are the values of the Poisson's ratio and the modulus of elasticity found from the relations (1) and (2) by utilizing the strain values obtained by solving a three-dimensional problem of the theory of elasticity at ν_0, E_0.

4. Results of determining the elastic constants of rock salt

Based on the results of numerical experiments for specimens with a length of 400 mm, the following dimensions were chosen: $b=60$ nm, $h=40$ mm ($L=300$ mm). When implementing the four-point bending scheme $l=L/2$. With these dimensions, the errors determining the fulfillment of the uniaxial stress state conditions, and the Bernoulli–Euler hypotheses, for Poisson's ratio values of $\nu = 0.05 \div 0.45$ will vary in the following ranges: $\beta_\nu = 0.3 \pm 0.1\%$, $\beta_{\text{Ä}} = 0.02 \div 0.1\%$. Considering the smallness of these values, the errors β_ν, β_E can be neglected when evaluating the obtained values of the elastic modulus and Poisson's ratio.

In the experiment, 10 specimens of rock salt made of a single plate mined at the Verkhnekamskoye potassium-magnesium salt deposit (Berezniki) were tested. Figure 2 shows the scheme of the four-point bending experiment, a specimen with fiber-optic sensors based on Bragg gratings, which are 5 mm long, glued along and across the length. During calibration tests using a high-precision linear positioner, the sensors demonstrated an error within 1–2%.

For Bragg grating sensors, the following relations satisfy [22]

$$\begin{aligned} \Delta\lambda_1/\lambda^* &= \varepsilon_3 - 0.5n^2(p_{11}\varepsilon_1 + p_{12}(\varepsilon_2+\varepsilon_3)), \\ \Delta\lambda_2/\lambda^* &= \varepsilon_3 - 0.5n^2(p_{11}\varepsilon_2 + p_{12}(\varepsilon_1+\varepsilon_3)), \end{aligned} \qquad (6)$$

where ε_3 is the strain along the optical fiber (measured strain), ε_1, ε_2 are the principal strains in the plane perpendicular to the optical fiber, p_{11}, p_{12} are the Pockels coefficients, $\Delta\lambda_1 = \lambda_1 - \lambda^*$, $\Delta\lambda_2 = \lambda_2 - \lambda^*$ are the resonant wavelengths shifts of the reflected spectrum between the deformed λ_1, λ_2 and non-deformed λ^* states (values measured by the sensor).

Fig. 2. (Color online) Universal four-point bending testing facility, fiber-optic sensors fixed on the sample surface, rock salt samples.

Under uniaxial stress state of the optical fiber $\varepsilon_1 = \varepsilon_2 = -\nu\varepsilon_3$, where ν — Poisson's ratio. In this case $\Delta\lambda_1 = \Delta\lambda_2 = \Delta\lambda$ and

$$\Delta\lambda/\lambda^* = \left(1 - 0.5n^2\left(p_{12} - \nu(p_{11} + p_{12})\right)\right)\varepsilon_3 \qquad (7)$$

or

$$\varepsilon_3 = 1/k \cdot \Delta\lambda/\lambda^*. \qquad (8)$$

An adhesive bond is used to fix the fiber-optic sensors, for which two options are possible. In the first option, the adhesive bond in the measurement zone is applied on the entire fiber, including the Bragg grating. In this case, a complex stress state with strain tensor components ε_1, ε_2, ε_3 exists in the sensor zone, and Eq. (8) is used to calculate the strains based on the assumption of a uniaxial stress-strain state in the Bragg grating. In the second variant of fixing the optical fiber with the Bragg grating on the specimen surface, the adhesive bond is absent in the Bragg grating zone, which allows for the justified use of Eq. (8). However, in this case, to measure negative strains, it is necessary to provide an initial strain ε_0 in the Bragg grating, which determines the maximum value of the measured negative strains. Experimental results with two options for fixing the fiber-optic sensors showed a difference in strain measurement results that almost coincides with the measurement error of the sensors used. In this regard, the second option was adopted for mass experiments.

Experimental results were obtained at different values of P (Fig. 1) with strain recorded both under applied load and after load removal. The strain measurement results for one specimen are presented in Table 1.

The presented results allow the conclusion that the material exhibits nearly elastic behavior within the implemented strain range.

To estimate the maximum error in determining the elastic modulus and Poisson's ratio, the results of strain measurements at loads $P = 300$ N were used. For this load, the values of the measured strains for different specimens are given in Table 2.

Based on the average strain values, for a strain measurement error of $\delta = 10^{-6}$, the maximum errors for the elastic modulus and Poisson's ratio were obtained: $\alpha_E = 10\%$, $\alpha_\nu = 23\%$.

Table 3 presents the statistical analysis results of the determined values of Young's moduli and Poisson's ratios for the studied type of rock salt.

5. Conclusions

A method for determining the elastic moduli and Poisson's ratios in compression and tension is presented, based on a variant of the four-point bending method for a beam with a rectangular cross-section.

Relations are provided for calculating the elastic moduli and Poisson's ratios in tension and compression for a bi-modulus material based on strain measurement results. Additionally, relationships for estimating the errors of the obtained elastic constants are presented, related to both the choice of specimen dimensions for four-point bending test and the inaccuracy of sensors when measuring of strains.

A strain measurement approach using fiber-optic Bragg grating sensors is described, with analysis of different options of sensor fixation on the specimen surface.

Results for determining elastic moduli and Poisson's ratios in tension and compression for rock salt, with analysis of error estimates based on the provided relations are presented. The obtained results provide a complete characterization of the quantitative values of the elastic constants and lead to the qualitative conclusion that, within measurement error, rock salt cannot be classified as a bi-modulus material.

Table 1. Results of strain measurements at different loads.

	P, N									
	100	0	150	0	200	0	250	0	300	0
$\varepsilon_x^+ \cdot 10^6$	7.68	−0.04	11.36	0.02	15.01	0.07	18.51	0.05	22.39	−0.08
$\varepsilon_x^- \cdot 10^6$	−7.26	−0.01	−10.82	−0.08	−14.41	−0.19	−17.96	−0.41	−21.59	−0.67

Table 2. Results of strain measurements under load P equals to 300 N.

	Specimen number (i)									
	$i=1$	$i=2$	$i=3$	$i=4$	$i=5$	$i=6$	$i=7$	$i=8$	$i=9$	$i=10$
$\varepsilon_x^+ \cdot 10^6$	23.73	24.80	20.11	24.14	20.88	22.20	21.33	18.76	18.48	20.25
$\varepsilon_y^+ \cdot 10^6$	−6.11	−7.92	−5.08	−7.00	−5.32	−5.51	−5.75	−4.16	−4.57	−5.77
$\varepsilon_x^- \cdot 10^6$	−22.50	−25.42	−19.43	−23.66	−20.04	−21.84	−22.43	−18.64	−17.86	−20.46
$\varepsilon_y^- \cdot 10^6$	5.98	5.35	5.12	6.49	4.39	5.55	4.89	4.32	4.33	4.50

Table 3. Results of statistical analysis.

	Average value	Confidence interval		Minimum	Maximum	Standard deviation
		from	to			
E^+, MPa	34180	32650	35710	31204	37068	2139
E^-, MPa	35297	33264	37330	29937	39209	2842
ν^+	0.263	0.248	0.278	0.225	0.297	0.022
ν^-	0.242	0.223	0.260	0.210	0.277	0.025

References

1. N.M. Proskuriakov, R.S. Permiakov, A.K. Chernikov, Physical and mechanical properties of salt rocks, Nedra, Leningrad, 1973, 272 p. (in Russian)
2. A.A. Bariakh, S.A. Konstantinova, V.A. Asanov, Deformation of salt rocks, UrO RAN, Ekaterinburg, 1996, 204 p. (in Russian)
3. V.G. Khloptsov, M.V. Semenova, D.V. Khloptsov, Mechanical properties of rock salt, Izhevsk Institute of Computer Research, Izhevsk, 2022, 104 p. (in Russian)
4. Z. Briševac, D. Pollak, A. Maričić, A. Vlahek, Modulus of elasticity for grain-supported carbonates — Determination and estimation for preliminary engineering purposes, Appl. Sci. 10 (2021) 6148.
5. D. Onalo, S. Adedigba, O. Oloruntobi, F. Khan, L. James, S. Butt, Data-driven model for shear wave transit time prediction for formation evaluation, J. Pet. Explor. Prod. Technol. 10 (2020) 1429–1447.
6. A.B. Petrovsky, V.Yu. Prushak, E.A. Lutovich, Physical and mechanical properties of the rocks of the Starobinsky deposit forming the Third potash layer and its roof, Doklady of the National Academy of Sciences of Belarus. 65 (2021) 484–494. (in Russian)
7. V.M. Zhigalkin, O.M. Usol'tceva, V.N. Semenov, P.A. Tsoi, V.A. Asanov, A.A. Bariakh, I.L. Pan'kov, V.N. Toksarov, Deformation of quasi-plastic salt rocks under different conditions of loading. Report I: deformation of salt rocks under uniaxial compression, J. Min. Sci. 41 (2005) 507–515.
8. B. Jiang, F. Ma, H. Gao, Q. Wang, S. Cai, C. Zhang, Z. Bian, G. Liu, The response mechanism and testing method of the rock elastic modulus while drilling, Geomatics, Nat. Hazards Risk. 15 (2024) 2354498.
9. I.L. Pankov, I.A. Morozov, Results of an experimental study of the effect of friction on the mechanical properties of salt rocks, Bulletin of PNRPU. Geology. Oil & Gas Engineering & Mining 16 (2017) 64–72.
10. I.L. Pankov, I.A. Morozov, The research into friction factor between the ends of specimens of varying heights and press plates on mechanical performance of salt rocks, News of the Higher Institutions. Mining Journal 2 (2015) 107–113. (in Russian)
11. Y. Zhang, D. Yu, Comparative study on the test method for tensile elastic modulus of rock materials, Adv. Civ. Eng. 2019 (2019) 3161953.
12. Y. Zhang, D. Yu, J. Ye, Study on measurement methodology of tensile elastic modulus of rock materials, Rock. Soil. Mech. 6 (2018) 2295–2303.
13. V.A. Asanov, I.L. Pankov, V.S. Kuzminyh, I.A. Morozov, The methodical aspects of strength, deformation and energy characteristic determination of salt rocks under direct tensile loading of rock specimens in laboratory conditions, PNRPU Mechanics Bulletin 4 (2018) 58–68. (in Russian)
14. I.L. Pankov, I.I. Garaeva, Study of mechanical properties of salt rocks under tension, MIAB 10 (2011) 87–90. (in Russian)
15. V.P. Efimov, The rock strength in different tension conditions, J. Min. Sci. 45 (2009) 569–575.
16. V.P. Efimov, Rock tests in nonuniform fields of tensile stresses, J. Appl. Mech. Tech. Phys. 54 (2013) 857–865.
17. A.A. Baryakh, N.A. Samodelkina, I.L. Pankov, Water-tight stratum rupture under large-scale mining. Part I, J. Min. Sci. 48 (2012) 771–780.
18. H. Bagheri, A.A. Tanha, F.D. Ardejani, M. Heydari-Tajareh, E. Larki, Geomechanical model and wellbore stability analysis utilizing acoustic impedance and reflection coefficient in a carbonate reservoir, J. Petrol. Explor. Prod. Technol. 11 (2021) 3935–3961.
19. N.A. Liadova, P.I. Klykov, A.A. Predein, Numerical solution of geomechanics problems (The case of the Baltic sea offshore field), Perm Journal of Petroleum and Mining Engineering 20 (2020) 126–136.
20. V.P. Matveenko, N.A. Kosheleva, G.S. Serovaev, A.Y. Fedorov, Measurement of gradient strain fields with fiber-optic sensors, Sensors 23 (2022) 410.
21. V.P. Matveenko, G.S. Serovaev, A.Y. Fedorov, E.B. Galkina, A.V. Zaitsev, Determination of elastic moduli and Poisson's ratios of bi-modulus materials based on the results of four-point bending test, Mater. Struct. 57 (2024) 96.
22. G. Luyckx, E. Voet, N. Lammens, J. Degrieck, Strain measurements of composite laminates with embedded fibre bragg gratings: Criticism and opportunities for research, Sensors. 11 (2010) 384–408.